IJAME

Int. J. of Applied Mechanics and Engineering, 2024, vol.29, No.3, pp.1-16
DOI: 10.59441/ijame/189957

COMPARING THE PERFORMANCE OF USING A SMART DAMPER IN A SEMI-ACTIVE SUSPENSION INSTEAD OF A TRADITIONAL DAMPER USING MATLAB/SIMULINK

Lamyaa Mahdi Ali* and Ali I. Al-Zughaibi

Department of Mechanical Engineering, College of Engineering, University of Baghdad, IRAQ,
E-mail: Lamiaa.Ali2303@coeng.uobaghdad.edu.iq

Given the importance of comfort and safety in various driving circumstances, the suspension system emerges as the most crucial component. Two different suspension systems, passive (PSS) and semi-active (SASS), are compared for effectiveness in this research. MATLAB/Simulink is used for simulation, employing a representative two-degree-of-freedom car model to evaluate and compare the performance results of these systems. The differential equations of motion for the two systems are modeled and simulated using software, which illuminates how they would behave under the same parameters and circumstances. Additionally, a Magnetorheological damper (MR) model with a ¼ vehicle system is used to evaluate its behavior on various types of roads, including those with steps, bumps, and random inputs. This study utilizes the Bingham plastic model to compare the simulation results of SASS and PSS systems. After comparing the numerical and graphical results from the two systems, it is observed that SASSs with controllers perform better than PSSs in terms of suspension adjustment and response time. The SASS is superior to the PSS in suppressing oscillations by *55.12*%, *77.47*%, and *86.78*% for step input, bump, and random inputs, respectively. Additionally, the SASS is faster in eliminating oscillations compared to the PSS by *54*% and *51.7*% for step input and bump inputs, respectively.

Key words: magnetorheological damper (MR), passive, quarter car, semi-active, system feedback controller.

1. Introduction

Both businesses and academia demonstrate significant interest in the chassis control of automobiles. A car must meet essential requirements like stability, safety, and driver comfort. Consequently, controlling vertical dynamics, achieved by regulating the car's suspension system, plays a crucial role in vehicle technology [1]. The primary objective of a vehicle's suspension system is to isolate the car from road irregularities, thereby enhancing road holding and driving comfort [2]. This system consists of three primary components: a damping element, various mechanical components, and an elastic component. While the suspension bears the entire static load, the elastic element applies force. Typically, a coil spring is used for this component. A shock absorber applies a dissipative force to the elongation speed, serving as the damping element. The mechanical element group connects the sprung body with the unsprung mass [3]. SASS represents a modern automotive suspension system with superior anti-roll, vibration damping, and vehicle stability effects. However, due to its intricate structure and distinct control mode, a popular area of research has focused on the control approach for SASS [4]. One type of intelligent substance used in these systems is Magneto-Rheological Fluid (MRF). Primarily behaving like a fluid, MRF can change its rheological properties from liquid to semi-solid (chain-like structure) within milliseconds when subjected to a magnetic field [5]. The magnetic field returns to its initial state after it disappears. The MRF's unique rheological properties are advantageous in mechanical devices such as clutches, brakes, and dampers [6]. In response to variations in the viscosity of the MRF under the influence of a magnetic field, an MR damper adjusts and regulates the damping

* To whom correspondence should be addressed

force. The automobile industry has recently shown interest in developing revolutionary vibration control techniques [7]. The MR damper in the SASS car suspension system is an example of advanced technology [8]. The unique reversible rheological property of the presents the most promising technological option for vibration reduction in a variety of applications, including protecting buildings against seismic events. When subjected to an external magnetic field, this characteristic results in a significant increase in viscosity [9]. There are applications for this technique in car suspension [10], the aircraft's landing gear system [11], as well as knee prosthesis [12]. This study replaces PSS with SASS employing MR dampers in an attempt to strike a difficult-to-achieve balance between handling and comfort. The objective is to perform significantly better in all areas. These methods explore how MR dampers, designed to reduce vibration and enhance system reliability, can be utilized to control an automobile suspension system. The goal is to enhance the comfort, safety, and performance of automotive occupants by researching and developing suspension systems to select the best one.

2. Passive suspension system

PSS, also known as traditional suspension, consists of dampers and springs. The PSS operates with an open-loop control system, serving a specific purpose. Its mechanical components cannot be modified due to their fixed nature. However, if a PSS is designed to be very firm or heavily damped, it may transmit a lot of road input or cause the vehicle to skid on uneven terrain. Conversely, if the suspension is supple or only lightly damped, it may be challenging for the vehicle to turn, change lanes, or sway. Therefore, the effectiveness of PSS depends on the road profile [13].

3. Semi-active suspension system

Many damping coefficients can be employed with SASS. It can only modify the shock absorber's viscous damping coefficient; they do not add energy to the suspension system and do not require frequent damper replacements. They use less energy to function and are more cost-effective. Due to their powerful dampening force, one intriguing type of SASS control device is the MR damper [13]. A damper, sometimes called a shock absorber, is a mechanical component that reduces kinetic energy and attenuates shock waves [14].

4. Mathematical models

A two-degree-of-freedom ¼ vehicle's SASS and PSS versions are shown in Fig.1 [15]. SASSs have a lot of promise in the automotive market because of their advantages over active and PSSs, particularly due to their low weight and cost-effectiveness. They also enhance vehicle performance [6].

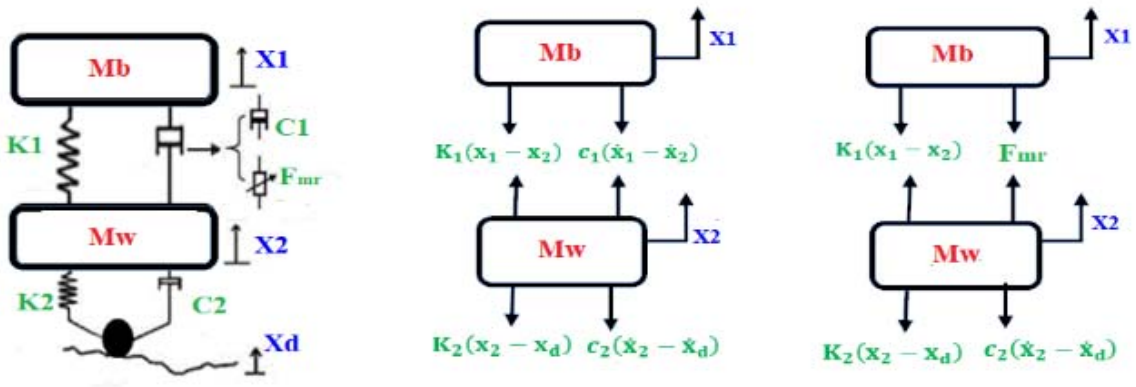

Fig.1. (a) Semi-active suspension model [1]. (b) Free body diagram for PSS. (c) Free body diagram for SASS.

Figure 1 shows the data representing the excitation caused by undesired road irregularities. It displays the mass of the vehicle body M_b, the total displacement of the body x_1, the equivalent stiffness of the suspension system k_1, the mass of the wheel M_w, the absolute displacement of the wheel x_2, the comparable stiffness of the wheel k_2, the zero-field damping coefficient of the suspension's magnetorheological resistor C_1, represent the total force exerted on the adjustable damping coefficient of the suspension's magnetorheological resistor F_{MR}, and the excitement caused by unwanted road imperfections x_d.The following mathematical equations can be used to express the movement of both masses using Newton's second law [2].

4.1. Passive suspension model

$$M_b\ddot{x}_1 = -k_1(x_1 - x_2) - C_1(\dot{x}_1 - \dot{x}_2), \tag{4.1}$$

$$M_w\ddot{x}_2 = -C_2(\dot{x}_2 - \dot{x}_d) - k_2(x_2 - x_d) + C_1(\dot{x}_2 - \dot{x}_1) + k_1(x_2 - x_1). \tag{4.2}$$

4.2. Semi-active suspension model

$$M_b\ddot{x}_1 = -k_1(x_1 - x_2) - F_{MR}, \tag{4.3}$$

$$M_w\ddot{x}_2 = -k_2(x_2 - x_d) - C_2(\dot{x}_2 - \dot{x}_d) + k_1(x_1 - x_2) + F_{MR}. \tag{4.4}$$

4.3. System parameters and conditions

Dynamic modeling was set up with the following conditions and parameters. The table provides parameters of a typical passenger car used in the MATLAB/Simulink simulated analysis [3].

Table 1. Simulation parameter PSS for a *1/4* vehicle [4].

Parameters	**Symbol**	**Values**	**Units**
Body mass	M_b	*241.5*	*Kg*
Wheel mass	M_w	*41.5*	*Kg*
Stiffness of the first spring	K_1	*6000*	*N /m*
Stiffness of the second spring	K_2	*14000*	*N /m*
The damping factor of the first damper	C_1	*1000*	*Ns /m*
The damping factor of the second damper	C_2	*1500*	*Ns /m*

5. MR damper

Key to the MR damper control mechanism is a hydraulic cylinder with particles suspended in a liquid that can be magnetically polarized. The way MR dampers work is by absorbing energy and dispersing vibration. MR fluid dampers combine the ease of use of active control systems with low power consumption and the dependability of PSSs to provide extremely effective vibration control. MRFs are used to provide a controllable damping force. Sometimes referred to as an MR shock absorber, this type of SASS control device dampens motion and controls vibrations using MR fluid [16], as illustrated in Fig.2.

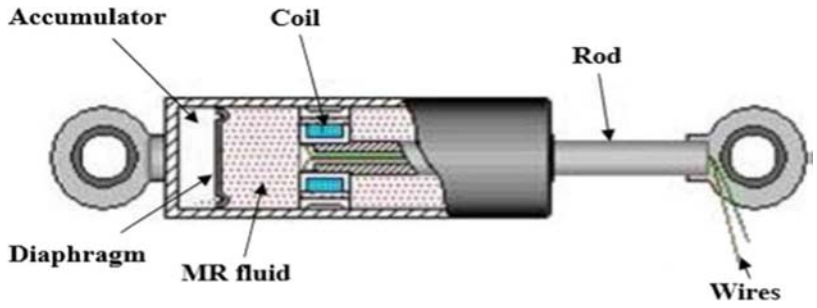

Fig.2. Structure of MR damper [5].

5.1. MR fluid

The ingenious material known as MR fluid can alter its viscosity in response to a magnetic field. The iron particles in the fluid organize themselves into chains that obstruct flow when a magnetic field is applied. Because of this change in viscosity, the MR damper can adjust its damping force in real time, providing better control over vibration and movement than conventional dampers [14], according to Fig.3.

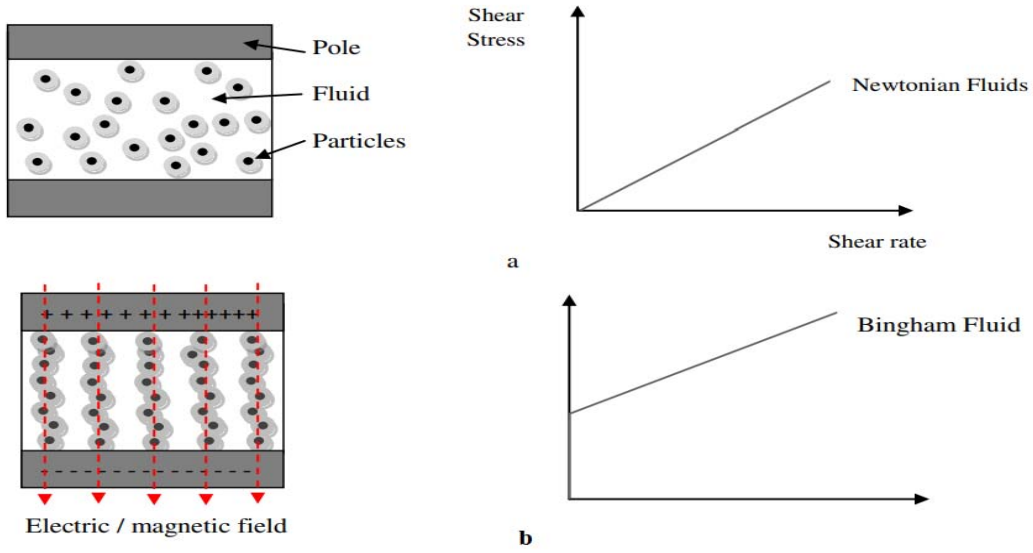

Fig.3. Mechanism of MR fluid effect [6]: (a) without magnetic field, (b) with magnetic field.

5.2. Models of the magneto-rheological damper

MR dampers are intricately designed devices with complex dynamics. Various models, with varying complexity and precision, have been developed to understand and predict their behavior. One type of MR damper model is clarified in our study, the simple Bingham model [17].

5.2.1. Model of Bingham-based-dynamic

The simplest model combines a viscous damper and a Coulomb friction element in parallel to explain the MR damper. It can accurately reproduce the force-displacement curves at low speeds, but it cannot replicate the hysteresis of the force-velocity curve. Due to its simplicity, it is commonly used for control design and preliminary analysis. It has a material response function MRF that comprises a Newtonian viscosity element

and a variably stiff, fully plastic element, defining the crucial relationship between stress and strain to be described in the following equations

$$\tau = \tau y(H)\operatorname{sgn}(\Upsilon) + \eta \tag{5.1}$$

where τ is the fluid's shear stress and τy is the yielding shear stress that is regulated by the applied magnetic field H represents the signum function, η represents the Newtonian fluid viscosity, and the shear strain rate is represented by. Stated otherwise, when the shear stress is less than the critical value τy, the fluid is at rest and behaves as a viscoelastic material. It then turns into a Newtonian fluid and begins to flow. The Bingham plastic model explains the field-dependent behavior of the yield stress [18], as depicted in Fig.4.

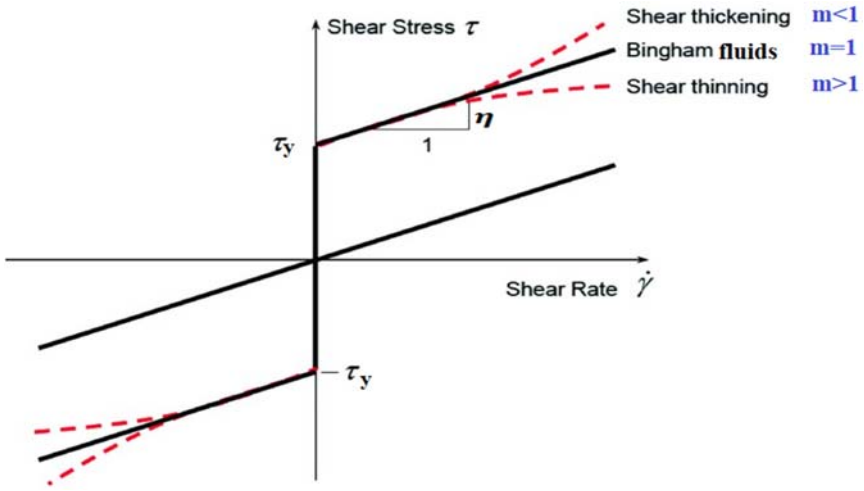

Fig.4. MR fluids are described using the Bingham plastic model [7].

As shown in Fig.5(a), the Bingham plastic model was developed by Stanway *et al.* [20]. It contained a Coulomb friction component that ran parallel to a viscous dashpot to characterize the electrorheological (ER) damping mechanism.

$$F_{MR} = F_C\, sgn + C_0\dot{x} + F_0\,, \tag{5.2}$$

where $\dot{x}$ denotes the velocity connected to external excitation, the damping parameter is C_0, the frictional force associated with the field-dependent yield Stress is denoted F_C, and The offset in the force applied is denoted by F_0.

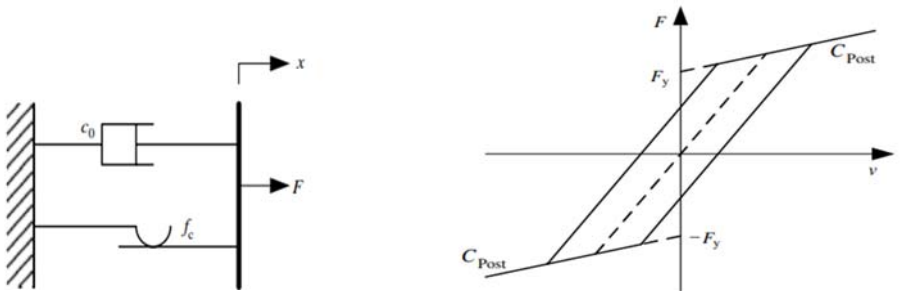

Fig.5. Bingham plastic model (a) a viscous dashpot parallel to a Coulomb friction element (b) the MR dampers piecewise continuous model [5].

The measured force has a nonzero mean to account for the accumulator's presence. It should be noted that the frictional force is equal to the applied force if the piston's velocity is zero at any moment. To see if it can forecast how the MR damper will behave, the Bingham behavior of an MR damper can be determined by using Eq.(5.2), which describes the Bingham plastic model for MRFs. After an MRF exceeds the yield point, its behavior can be explained using the Bingham model. Typically, this requires full fluid flow and high shear rates. However, the model assumes that the fluid is rigid in this region before it reaches the yield point. Therefore, the Bingham model does not accurately describe the fluid's elastic characteristics for small deflections and low shear rates in dynamic applications. Since the model's inception, numerous studies in the field have attempted to enhance the fundamental Bingham model, This defines the behavior of MR dampers to enhance the predicted hysteretic cycle. It is also possible to represent the damping force for MRDs using the nonlinear Bingham plastic model [15]. Figure 5(a) illustrates the force generated by the MRDs.

By fitting the Bingham model to the *2.5 Hz* sinusoidal response data for the scenario where the command voltage to the current driver is a constant *1.5 V*, the predictive capability of the model for the behavior of the MR damper was assessed. The chosen parameters are shown in Fig.7.

Table 2. The Bingham model's parameter values [19].

Parameter	Value
F_C	*670 N*
C_0	*50 N s/cm V*
F_0	*-95 N*

MATLAB/Simulink simulates the Bingham model, as shown in Fig.6, using the parameters provided in Tab.2.

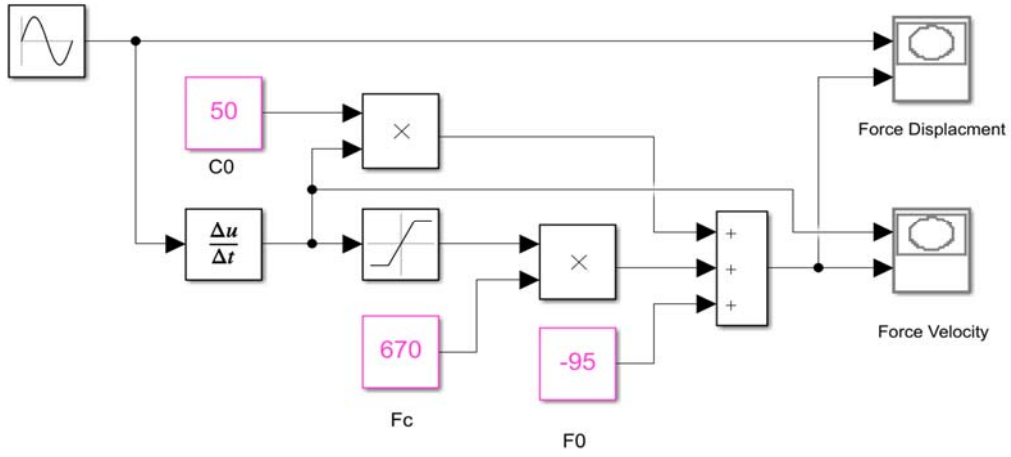

Fig.6. Bingham model simulation with MATLAB/Simulink.

The hysteresis effect of the MR damper is seen in Fig.7, Different forces are generated depending on whether the displacement is positive or negative. Viscoelastic behavior is displayed by MR fluids in the presence of an external shear force applied perpendicular to the magnetic field. The polarization chains' ability to tolerate some shear stress explains this. Pre-yield region is the term used to describe this area. The polarization chains will break when the external shear stress rises over a specific point, converting MR fluids into standard Newtonian fluids. This region is known as the post-yield region. Hysteresis results from the polarization chains being linked up by the steadily decreasing shear stress. Still, compared to before the break in the polarization chains occurs, less stress is needed to complete the link [8]. When the velocity is zero, the

force measured is positive; when the acceleration is negative (a positive displacement), it is negative; and when the acceleration is positive (a negative displacement), the measured force is negative.

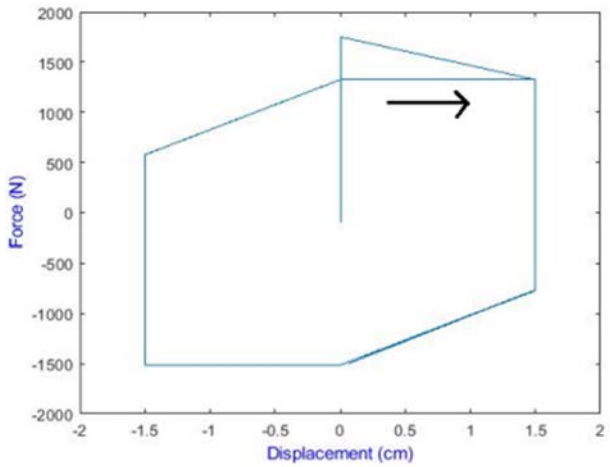

Fig.7(a). Displacement-force diagram derived from the Bingham model.

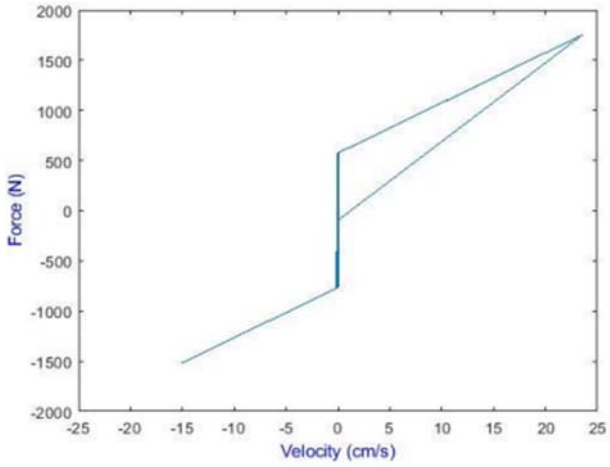

Fig.7(b) Diagram of velocity and force derived from the Bingham model.

6. Modelling suspension systems in Matlab Simulink

6.1. Method of passive suspension

Using Eqs (4.1-4.2), the code can be seen in the figure. A model, denoted as 9, is developed in the MATLAB/Simulink environment to analyze the system's response. A block diagram representing the PSS in Fig.8 [21] includes the vehicle's body mass, road disturbance, and suspension system.

Fig.8. Block schematic of the PSS [9].

6.2 Method of semi-active suspension system / Bingham model

By creating a simulation code, the parametric model/Bingham used in this paper will be simulated. Without a damper control unit, the MR damper will be assumed to operate at a constant voltage. By entering the damping force with a different sign on each spring and non-spring mass in Eq.(5.2), the Bingham model predicts the damping force that results from the MR damper. Using the Simulink environment, Fig.10 displays the simulation code of the Bingham model in the equation of motion for the two-car models [22].

7. Results and discussion

This section compares SASS and PSS analyses, emphasizing the behavior and advancements of SASS models (such as the simple Bingham model) after their introduction to the ¼ car model and subsequent exposure to various forms of road disturbance profiles.

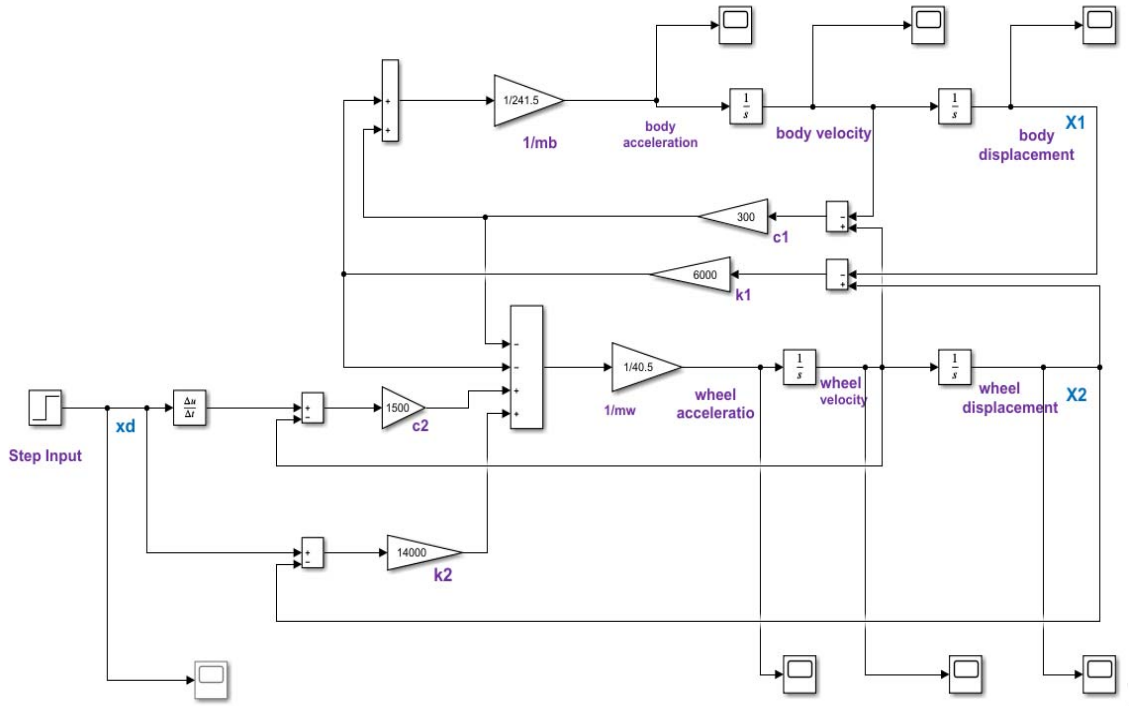

Fig.9. Simulink model for the PSS.

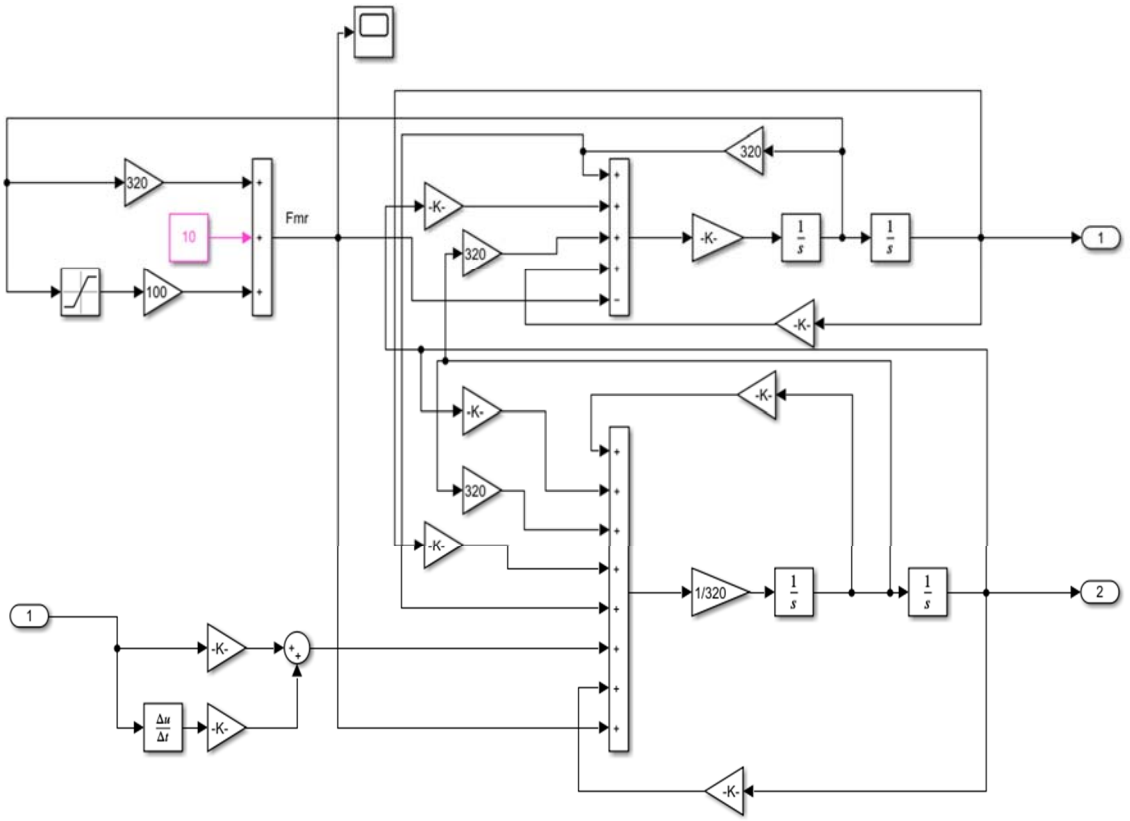

Fig.10. Bingham model simulation with MATLAB/Simulink embedded in SASS control [10].

7.1. Step input road profile (1)

The following results compare PSS and SASS responses when subjected to the first type of road disturbance profile 1 (step input), as illustrated in Figs 11-13.

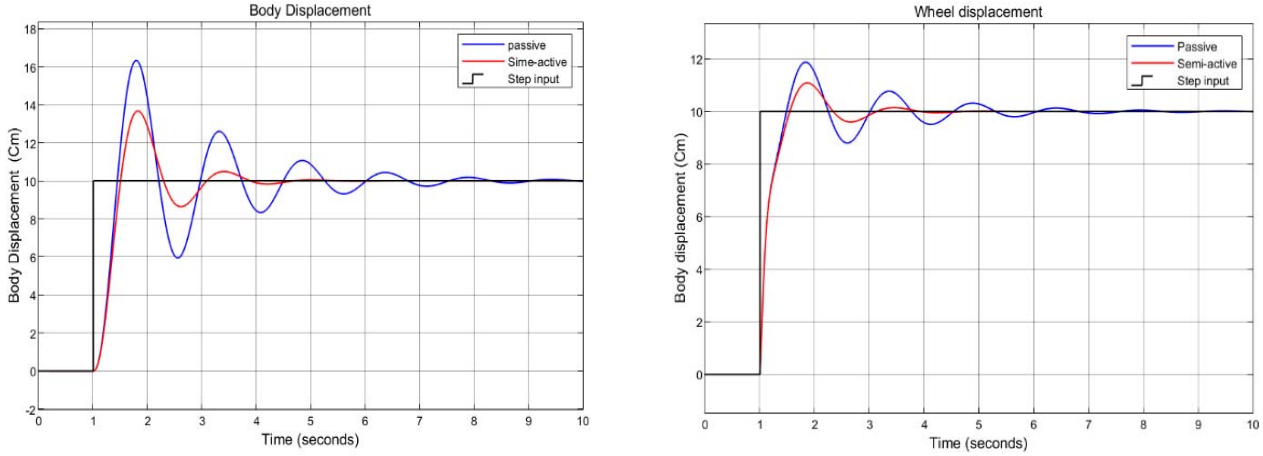

Fig.11. Comparison of SASS and PSS (body-wheel-displacement-step input).

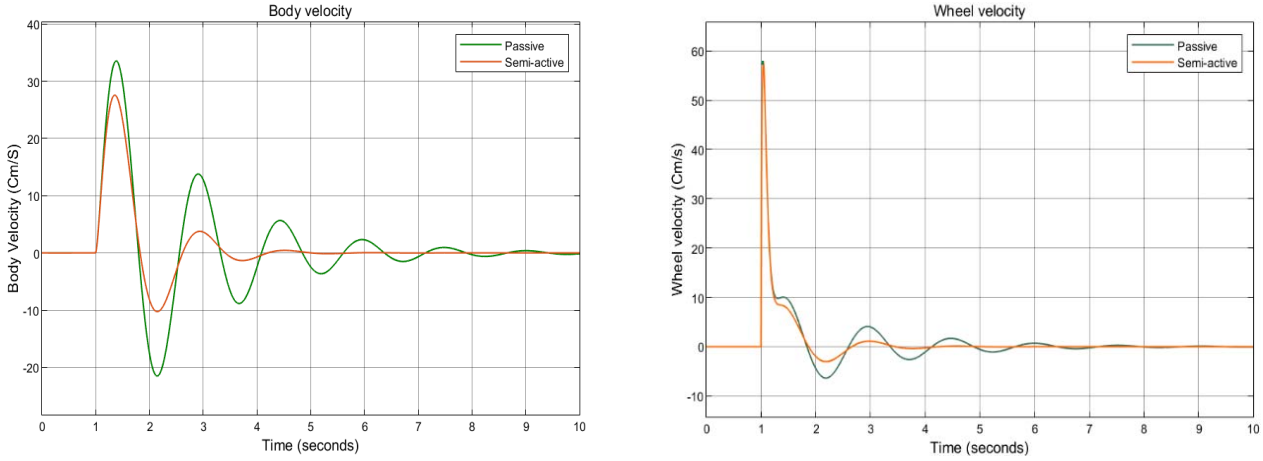

Fig.12. Comparison of SASS and PSS (body-wheel-velocity-step input).

SASSs enable cars to absorb initial impacts more effectively by adjusting their damping qualities in response to road irregularities. This is demonstrated when a car with SASS is exposed to a step-input road disturbance and its simulated displacement for both the body and wheel is compared to that of the PSS.

1. The results indicate that the SASS is superior to the PSS in suppressing oscillations by *55.102*%.
2. The SASS is *54*% faster at eliminating oscillations compared to the PSS, as shown in the Tab.3.

Table 3. The difference between body and wheel mass displacement-step input function.

Type of suspension systems	Passive	Semi-active	Passive - semi-active improvement (%)
The differences in mass displacement between sprung and unsprung	*4.9 Cm*	*2.2 Cm*	*55.102 %.*
Stabilizing time	*10 s*	*4.6 s*	*54 %*

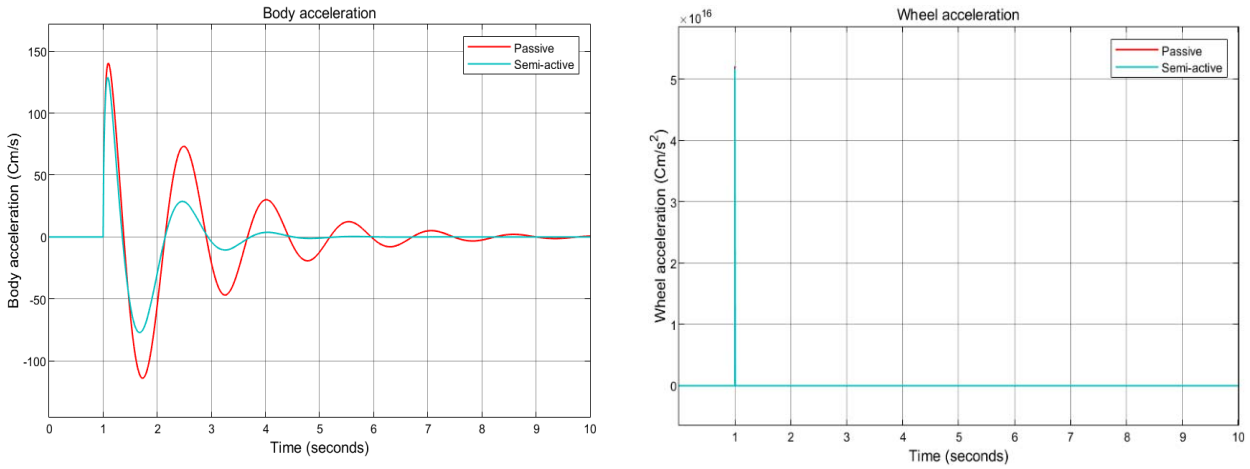

Fig.13. Comparison of SASS and PSS (body-wheel-acceleration-step input).

SASSs enable cars to absorb initial impacts more effectively by adjusting their damping qualities in response to road irregularities. This is demonstrated when a car with SASS is exposed to a step-input road disturbance and its simulated displacement for both the body and wheel is compared to that of the PSS.

1. The results indicate that the SASS is superior to the PSS in suppressing oscillations by *55.102*%.
2. The SASS is *54*% faster at eliminating oscillations compared to the PSS, as shown in the Tab.3.

Table 3. The difference between body and wheel mass displacement-step input function.

Type of suspension systems	**Passive**	**Semi-active**	**Passive - semi-active improvement (%)**
The differences in mass displacement between sprung and unsprung	*4.9 Cm*	*2.2 Cm*	*55.102 %.*
Stabilizing time	*10 s*	*4.6 s*	*54 %*

7.2. Bump road profile (2)

The road disturbance bump is illustrated in Fig.14. The following results compare PSS and SASS when they are exposed to the second type of road disturbance profile 2 (bump), as shown in Figs 15-17.

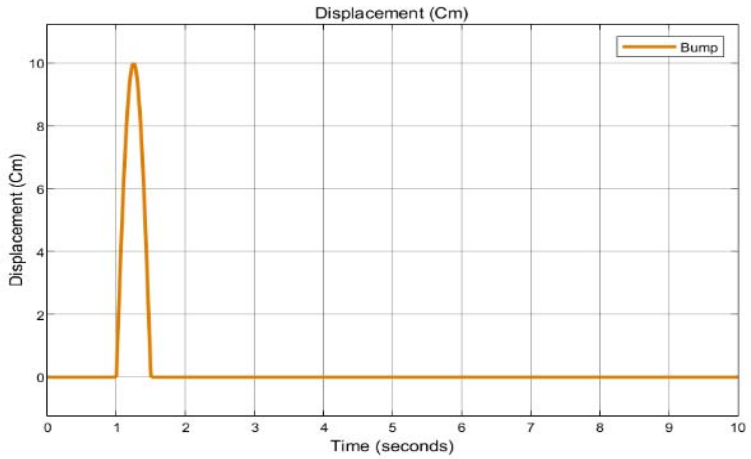

Fig. 14. Road disturbance bump profile (2).

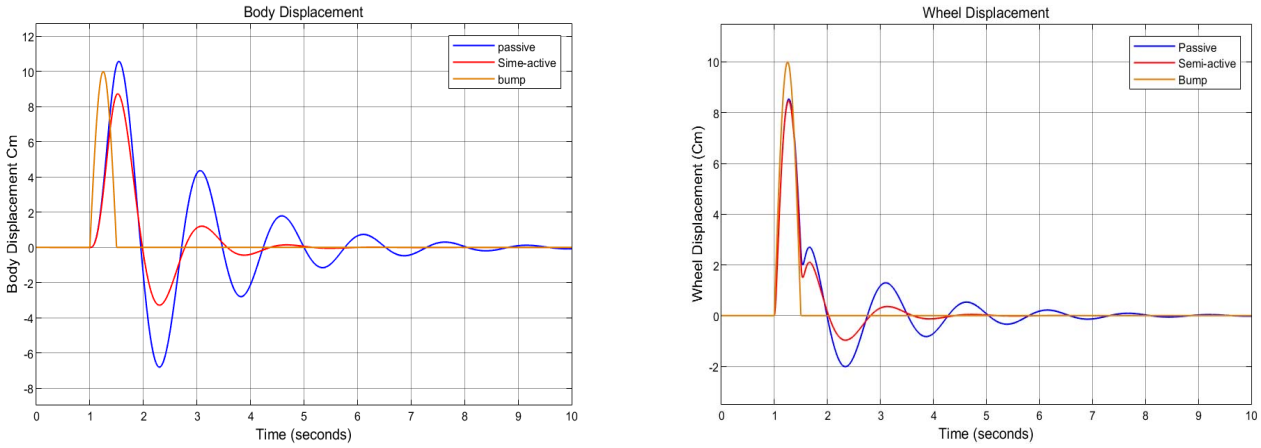

Fig.15. Comparison of SASS and PSS (body-wheel-displacement-bump).

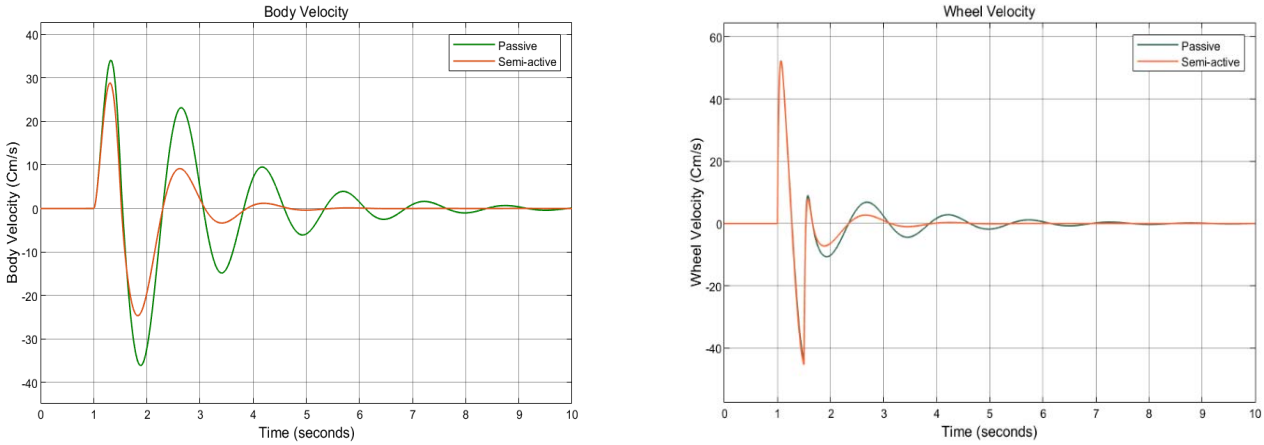

Fig.16. Comparison of SASS and PSSs (body-wheel-velocity-bump).

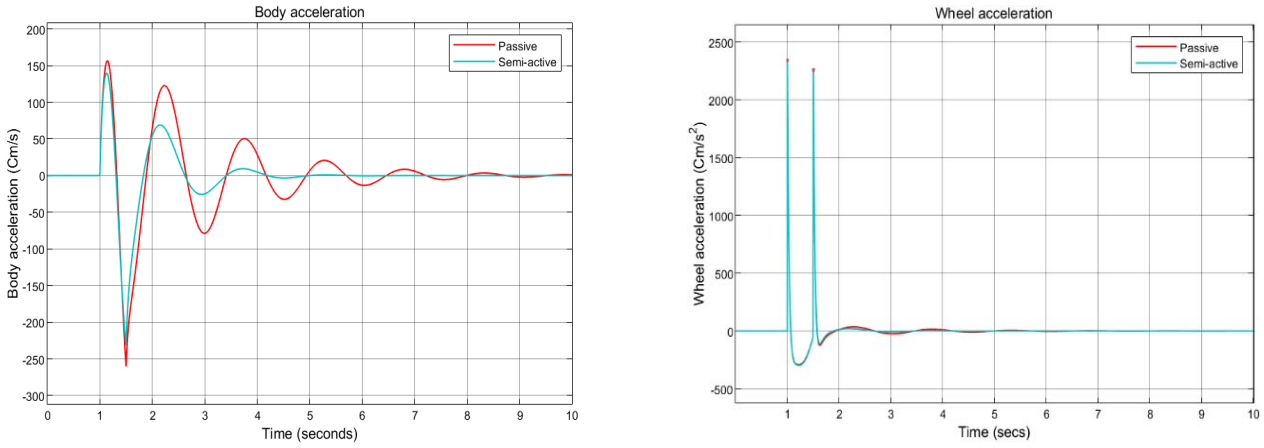

Fig.17. Comparison of SASS and PSSs (body-wheel-acceleration-bump).

Comparing the simulated displacement of the sprung and unsprung masses of a car under bump road disturbances using SASS and PSS shows a reduced peak displacement in SASS. This reduction effectively decreases the peak displacement of the sprung mass (vehicle body) compared to PSS, functioning similarly to a step input. The degree of reduction may vary slightly depending on the shape and length of the bump.

1. The results indicate that the SASS is superior to the PSS in suppressing oscillations by *77.47*%.
2. The SASS is *51.7*% faster at eliminating oscillations compared to the PSS as demonstrated in Tab.4.

Table 4. The difference between body and wheel mass displacement-bump input function.

Type of suspension systems	**Passive**	**Semi-active**	**Passive - semi-active improvement (%)**
The differences in mass displacement between sprung and unsprung	*2.22 Cm*	*0.5 Cm*	*77.47 %*
Stabilizing time	*10 s*	*4.83 s*	*51.7 %*

7.3. Random road profile (3)

The randomness of road disturbances is illustrated in Fig.18 [24].
The following results compare PSS and SASS when exposed to the third type of road disturbance profile 3 (Random), as shown in Figs 19-21.

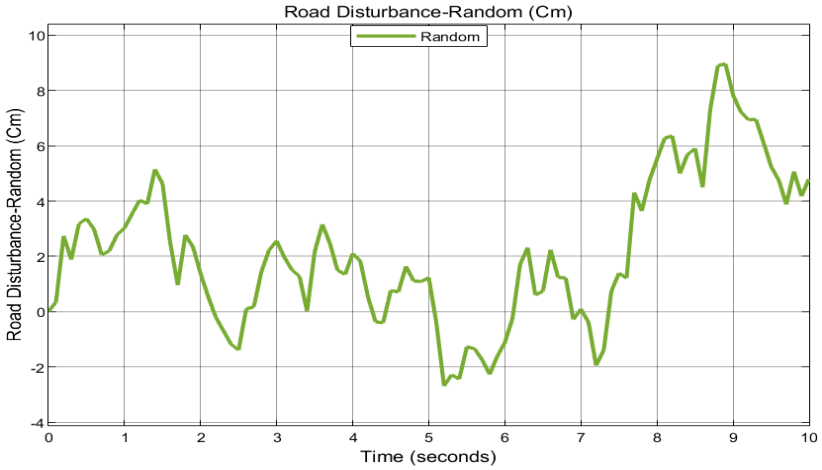

Fig.18. Road disturbance random profile (3).

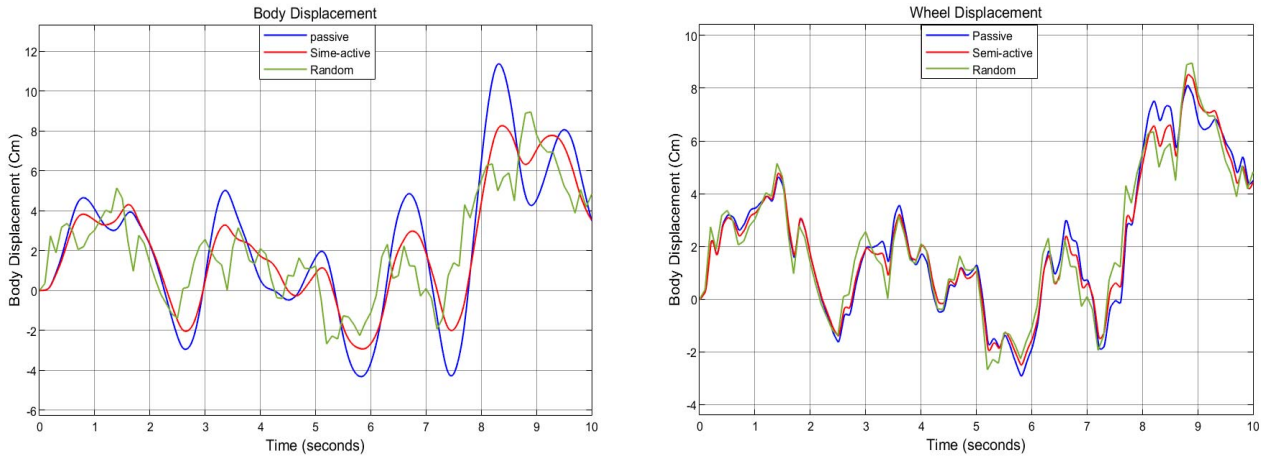

Fig.19. Comparison of SASS and PSSs (body-wheel-displacement-random).

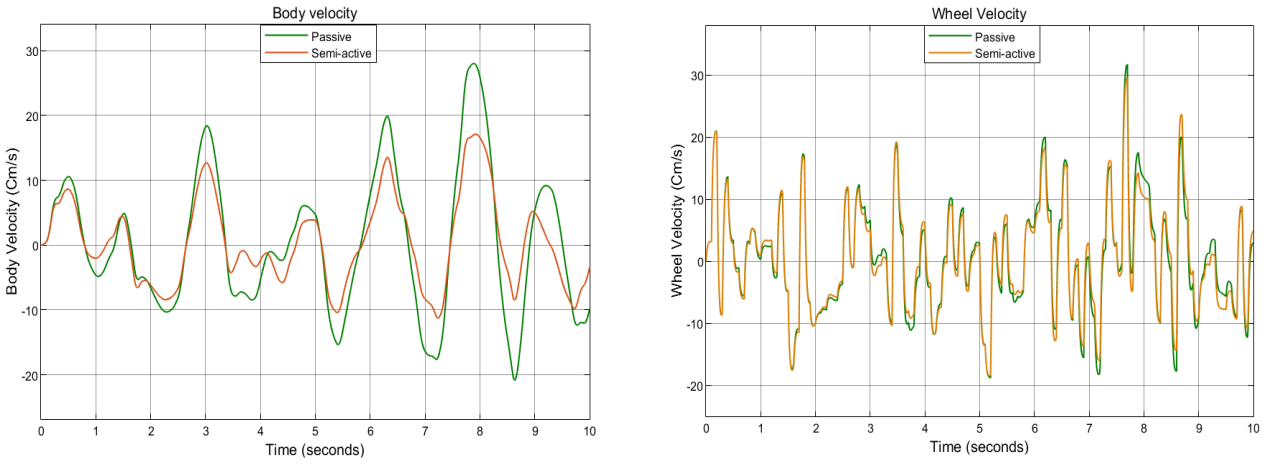

Fig.20. Comparison of SASS and PSS (body-wheel-velocity-random).

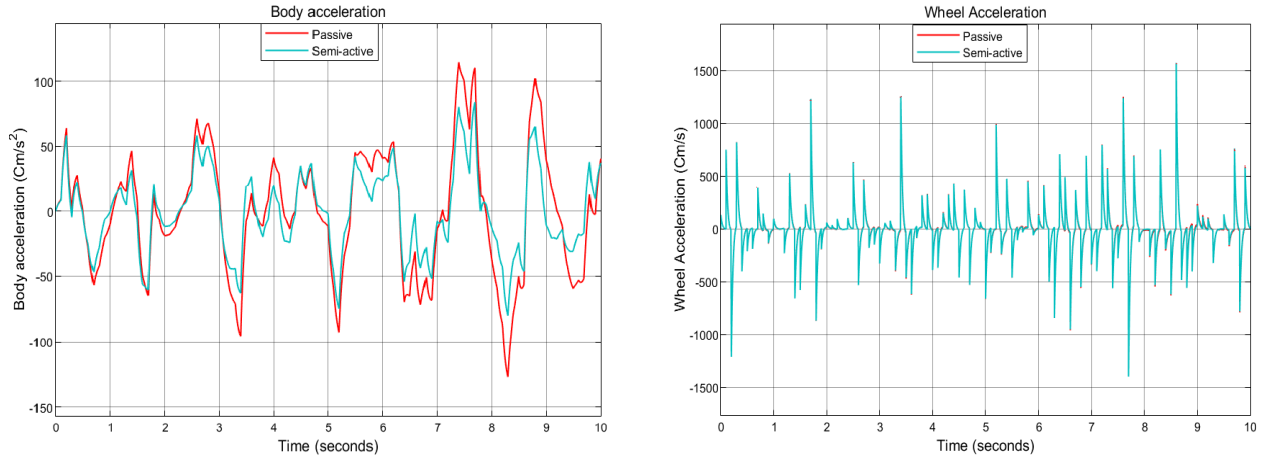

Fig.21. Comparison of SASS and PSS (body acceleration-random).

In general, SASS continues to offer advantages over PSS when dealing with more complex scenarios involving simulating the displacement of a vehicle under random road disturbances. SASS suspensions generally exhibit a significant reduction in Root Mean Square (RMS) displacement compared to PSSs. However, accurately predicting the peak displacement for each bump within the random profile is challenging. This indicator corresponds to a smoother ride quality and represents the total "roughness" that the car experiences.

1. The results indicate that the SASS is superior to the PSS in suppressing oscillations by *86.78*% as shown in Tab.5.

Table 5. The difference between body and wheel mass displacement- random input function.

Type of suspension systems	**Passive**	**Semi-active**	**Passive - semi-active improvement (%)**
The differences in mass displacement between sprung and unsprung	*2.8 Cm*	*0.37 Cm*	*86.78 %*

Similar patterns of displacement can be observed when comparing the simulated acceleration and velocity responses of a car with the SASS and PSS to various road disturbance inputs.

8. Conclusion

The research assesses the control capability of the MR suspension system under various driving circumstances. Comparing the SASS of a passenger car to a PSS, the controller design technique developed for the system allows the SASS to outperform the PSS in achieving design objectives. A two-degree-of-freedom automobile model has been utilized for the mathematical modeling of both PSS and SASS systems.

1. According to the simulation results, in SASS, MR dampers provide several benefits, including adaptable damping. The main advantage is that the damping force can be dynamically adjusted in real-time based on various parameters such as driving style, vehicle speed, and road conditions. This feature enhances comfort on straight highways by providing a softer ride. It also automatically adjusts damping on rough terrain or during hard maneuvers to enhance handling and stability.
2. The major advantages of using SASS over PSS include the near-total elimination of system oscillations, reduction in the magnitude of oscillatory phenomena, and shorter disruptive periods.
3. For enthusiasts or vehicles that require more precise handling and comfort optimization, SASS is the best option.

Ultimately, the simulation results demonstrate the superior performance of the SASS.

ACKNOWLEDGMENT

The author expresses gratitude to the entire team of the Mechanical Engineering Department at the College of Engineering, University of Baghdad, for their invaluable help and guidance.

Nomenclature

C_1 – suspension damping coefficient $[N\,s/m]$

C_2 – tire damping coefficient $[N\,s/m]$

F_{MR} – damper force $[N]$

M_b – body mass/sprung mass $[kg]$

M_w – wheel mass/un-spring mass $[kg]$

k_1 – suspension spring coefficient $[N/m]$

k_2 – tire spring coefficient $[N/m]$

x_d – road profile displacement $[m]$

x_1 – vertical body displacement $[m]$

x_2 – vertical wheel displacement $[m]$

$\dot{x}_1$ – body mass velocity $[m/s]$

$\dot{x}_2$ – wheel mass velocity $[m/s]$

$\ddot{x}_1$ – body mass acceleration $\left[m/s^2\right]$

$\ddot{x}_2$ – wheel mass acceleration $\left[m/s^2\right]$

References

[1] Al-Ashtari W. (2023): *Fuzzy logic control of active suspension system equipped with a hydraulic actuator*.– Int. J. Appl. Mech. Eng., vol.28, No.3, pp.13-27, doi: 10.59441/ijame/172895.

[2] Al-Araji H.M.H., Al-Zughaibi A.I.H. and Hussein E.Q. (2023): *Testing two types of magneto-rheological (MR) damper models with quarter car suspension system response*.– Int. J. Tech. Phys. Probl. Eng., vol.15, No.1, pp.52-61.

[3] Wu J., Yang D., Cao W., Sun J., Wang Y. and Cao W.Z. (2023): *Simulation study of semi-active suspension fuzzy adaptive PID control system*.– J. Phys. Conf. Ser., vol.2501, No.1, doi: 10.1088/1742-6596/2501/1/012040.

[4] Bhise A.R., Desai R.G., Yerrawar M.R.N., Mitra A.C. and Arakerimath D.R.R. (2016): *Comparison between passive and semi-active suspension system using Matlab/Simulink*.– IOSR J. Mech. Civ. Eng., vol.13, No.04, pp.01-06, doi: 10.9790/1684-1304010106.

[5] Kumar S., Medhavi A., Kumar R., and Mall P.K. (2022): *Modeling, analysis and PID controller implementation on suspension system for quarter vehicle model*.– Journal of Mechanical Engineering and Sciences, vol.16, No.2., pp.8905-8916, doi: 10.15282/jmes.16.2.2022.08.0704.

[6] Sinjari S. (2023): *Comparing Optimization Algorithms for Parameter Identification of Sigmoid Experimental Study on The Behaviour of a Magnetorheological (MR) Damper and Evaluation of Numerical Models*.– Electronic Theses and Dissertations, University of Windsor, https://scholar.uwindsor.ca/etd/9309

[7] Silva D.M.D., Avila S., Morais M.V.G. and Cavallini A.A. Jr (2023): *Comparing optimization algorithms for parameter identiication of sigmoid model for MR damper comparing optimization algorithms for parameter identification of sigmoid model for MR damper*.– No.6, doi: 10.21203/rs.3.rs-2898815/v1.

[8] Sassi S., Sassi A., Cherif K. and Tarlochan F. (2018): *Magnetorheological damper with external excitation for more efficient control of vehicles dynamics*.– J. Intell. Mater. Syst. Struct., vol.29, No.14, pp.2919-2932, doi: 10.1177/1045389X18781038.

[9] Braz-Cesar M.T. and Barros R.C. (2010): *Semi-active vibration control of buildings using MR dampers : numerical and experimental verification*.– 14th Eur. Conf. Earthq. Eng., p.829.

[10] Pepe G., Roveri N. and Carcaterra A. (2019): *Experimenting sensors network for innovative optimal control of car suspensions*.– Sensors (Switzerland), vol.19, No.14, pp.14-17, doi: 10.3390/s19143062.

[11] Kang B.H., Jo B.H., Kim B.G., Hwang J.H. and Choi S.B. (2023): *Linear and nonlinear models for drop simulation of an aircraft landing gear system with MR dampers*.– Actuators, vol.12, No.7, doi: 10.3390/act12070287.

[12] Ochoa-Diaz C., Rocha T.S., Oliveria L.L. and Paredes M.E. (2014): *An above-knee prosthesis with magnetorheological variable-damping*.– Proc. IEEE RAS EMBS Int. Conf. Biomed. Robot. Biomechatronics, No.8, pp.108-113, doi: 10.1109/biorob.2014.6913761.

[13] Abdul Aziz M., Muhtasim S. and Ahammed R. (2022): *State-of-the-art recent developments of large magnetorheological (MR) dampers*.– Korean Society of Rheology, Australian Society of Rheology, vol.34, No.2, doi: 10.1007/s13367-022-00021-2.

[14] Zhang Y., Guo J., Yang J. and Li X. (2023): *Recent structural developments and applications of magnetorheological dampers (MRD): a review*.– Magnetochemistry, vol.9, No.4, doi: 10.3390/magnetochemistry9040090.

[15] Elderrat H.I. (2013): *Research Towards the Design of a Novel Smart Fluid Damper Using a McKibben Actuator*.– Submitted for the degree of Master of Philosophy, University of Sheffield, p.65.

[16] Kim B.G., Yoon D.S., Kim G.W., Choi S.B., Tan A.S., and Sattel T. (2020): *Design of a novel magnetorheological damper adaptable to low and high stroke velocity of vehicle suspension system*.– Appl. Sci., vol.10, No.16, doi: 10.3390/app10165586.

[17] Zhang S., Shi W., and Chen Z. (2021): *Modeling and parameter identification of MR damper considering excitation characteristics and current*.– Shock Vib., vol.2021, No.3, doi: 10.1155/2021/6691650.

[18] Yang G., Spencer B.F., Carlson J.D. and Sain M.K. (2002): *Large-scale MR fluid dampers: modeling and dynamic performance considerations*.– Eng. Struct., vol.24, No.3, pp.309-323, doi: 10.1016/S0141-0296(01)00097-9.

[19] Wang D.H. and Liao W.H. (2011): *Magnetorheological fluid dampers: a review of parametric modelling*.– Smart Mater. Struct., vol.20, No.2, doi: 10.1088/0964-1726/20/2/023001.

[20] Spencer Jr B.F., Dyke S.J., Sain M.K. and Carlson J.D. (1996): *Phenomenological model of a magnetorheological damper*.– J. Eng. Mech., vol.230-238, No.123, pp.1-23, doi: 10.1061/(ASCE)0733-9399(1997)123.

[21] Jamil M., Zafar S., and Gilani S.O. (2018): *Designing PID controller based semi-active suspension system using MATLAB simulink*.– Lect. Notes Inst. Comput. Sci. Soc. Telecommun. Eng. LNICST, vol.224, No.7, pp.282-295, doi: 10.1007/978-3-319-94180-6_27.

[22] Riazi B. (2021): *Design and Investigation of a Semi-Active Suspension System in Automotive Applications*.– Electronic Theses and Dissertations, University of Windsor, https://scholar.uwindsor.ca/etd/8683

[23] Eshkabilov S. (2016): *Modeling and simulation of non-linear and hysteresis behavior of magneto-rheological dampers in the example of quarter-car model*.– Engineering Mathematics, vol.1, No.1, pp.19-38, doi: 10.11648/j.engmath.20160101.12.

[24] Ismaili N. (2019): *Performance analysis of passive, semi-active and active-controlled suspension systems using MATLAB / SIMULINK*.– Journal of Applied Sciences-Sut, vol.5, No.9, pp.94-105.

Received: April 29, 2024
Revised: June 12, 2024